Collective modes in a saturated lithium-ammonia solution as a probe of the response of the low-density homogeneous electron gas

C. Petrillo,[1,2] F. Sacchetti,[1,2] E. Guarini,[2,3] L. E. Bove,[4] and F. Demmel[5,*]

[1]*Dipartimento di Fisica, Università di Perugia, I-06123 Perugia, Italy*
[2]*Consiglio Nazionale delle Ricerche, Istituto Officina dei Materiali, I-34149 Trieste, Italy*
[3]*Dipartimento di Fisica e Astronomia, Università di Firenze, I-50019 Sesto Fiorentino, Italy*
[4]*Département Physique des Milieux Denses CNRS-IMPMC, Université Paris 6, F-750175 Paris, France*
[5]*Institut Laue Langevin, B.P. 156, F-38042 Grenoble Cedex 09, France*

The ion dynamics of a saturated lithium ammonia solution was investigated by inelastic neutron scattering with optimized resolution. The experimental dispersion curve and mode damping, here carefully probed in a wave-vector range extending well below and above 1 Å^{-1}, display visible anomalies around 0.8 Å^{-1}. We relate the dispersion relation anomaly to the shape of the electron gas dielectric function, which screens the ion-ion potential in a way peculiar of the low electron density of the system. The increase of the damping around 0.8 Å^{-1} also supports the presence of a new decay channel for the collective excitations. An interpretation of these effects, based on the low electron-density properties of the lithium-ammonia solution, is proposed.

I. INTRODUCTION

The behavior of the homogeneous electron gas is still one of the most challenging problems relevant to all condensed-matter systems. This problem has been addressed in the past using various theoretical approximations.[1,2] In more recent times, modern quantum Monte Carlo (QMC) simulations have provided useful estimates of the electron-gas energy, pair correlation function, and other ground-state properties,[3] which serve as a reference for formal theoretical approaches.

Experimental ways to access the properties of the electron fluid are few. However, both structural[4] and dynamic[5,6] properties related to density fluctuations of the ions of a liquid metal can be taken as probes of the electronic response function. An important point in this investigation method is that, in the limit of point-like ions embedded in a homogeneous electron gas, the linear response assumption corresponds to the existence of *harmonic* collective and high-frequency modes which propagate with a velocity c such that[6] $c^2 = \Omega_p^2/k_s^2$, where Ω_p is the ion plasma frequency and k_s is the screening wave vector of the electron gas. The linear response regime for a real liquid is generally considered to be appropriate.[7] Nonetheless, the actual shape of the ion-ion potential introduces anharmonic effects and also *phonon* interactions, related to structural relaxations and disorder always present in liquids, may play a role. Interestingly, the simple formula for c is able to qualitatively describe the collective mode velocity of different liquid metals.[5]

It is worth recalling that the low-density electron gas is characterized by a well-known anomaly related to the occurrence of a negative compressibility at densities $n = 3/[4\pi(r_s a_0)^3]$ smaller than the critical density n_c,[1] corresponding to $r_s^{(c)} = 5.45$.[8] Beyond the critical region, the compressibility sum rule[1] implies the (static) dielectric function to be negative and a perturbation charge *overscreening* occurs. This point has been the subject of various investigations to confirm its physical consistency.[9,10] Differently, the random phase approximation (RPA) predicts a positive dielectric function at any density[1] and only more accurate descriptions[11,12] can provide the correct

behavior. Therefore there is a clear drawback in the simple formula for c since k_s^2 becomes negative when the density is smaller than n_c, while *undercritical-density* systems exist in nature which exhibit clear signatures of collective modes propagation, e.g., liquid Cs.[13]

Here we inquire into the case of the electron gas at low density, with neutron scattering measurements of the ion dynamics of the saturated lithium-ammonia solution, a natural metallic liquid having an electron density quite smaller than the usual metallic ones, i.e., characterized by $r_s = 7.4$, markedly exceeding $r_s^{(c)}$.

Recent x-ray and neutron inelastic scattering experiments[6,14,15] on this system have shown that *long-living* ion density fluctuation modes exist, with a dispersion curve which seems to be dramatically affected by the electron-electron interactions governing the electron-gas behavior at low density. A Kohn-like anomaly[6,14] was invoked to explain the pronounced kink visible in the experimental dispersion curve at $Q \simeq Q_a = 0.8$ Å^{-1}.

Given the limited information available on the response of the low-density electron gas, and the few experimental investigations performed in real systems[4] which mimic such a subtle system, we carried out more accurate neutron experiments on the saturated lithium-ammonia solution. The neutron technique is particularly suited to determinations of the dynamics of the whole Li(ND$_3$)$_4$ complex thanks to the preferential coupling of the probe with the deuterium atoms. Our main goal was to properly scan, with better energy resolution, the important Q range where the anomaly develops, with measurements extending also well above 0.8 Å^{-1}, that is a Q value very close to twice the Fermi wave vector where the anomaly was previously observed.

II. EXPERIMENT AND DATA MODELING

The present experiment was performed by using the IN8 three-axis spectrometer of the Institut Laue Langevin

(Grenoble, France) with a constant analyzer final energy of ∼35 meV and a high-resolution setup. The elastic energy resolution was calculated[16] to have a full width at half maximum (FWHM) of 1.05 meV, in agreement with that experimentally derived from the incoherent elastic scattering of a vanadium plate. The dynamics of the saturated (20 mole % metal) sample solution at $T = 220$ K was investigated at eleven Q values between 0.2 and 2.0 Å^{-1}. The experimental procedure and the data treatment were the same as those described in Ref. 6 and consisted of the subtraction of the background, by accurately taking into account the sample attenuation, and of the multiple scattering signal, simulated as for the previous experiment performed in similar conditions.[6]

The correct dynamic structure factor $S(Q,\hbar\omega)$ is shown in Fig. 1 at five selected Q values. It is quite evident from the experimental data that at low Q well-defined collective modes propagate in the system, as it was found in the previous investigations by x-ray[14,15] and neutron[6] scattering. Upon increasing Q, $S(Q,\hbar\omega)$ becomes less structured even

FIG. 1. Experimental $S(Q,\hbar\omega)$ of the saturated lithium ammonia solution, at selected Q values (full circles). Error bars compare with the symbol size. Solid lines are the best-fit curves according to the model of Eq. (1). The thin solid lines represent the DHO contribution. In each frame, the upper curves are a zoom (×5) of the spectrum tail.

if rather intense inelastic wings continue to exist. Therefore, to get more physical information an empirical fitting model was employed. The empirical and quite effective data-fitting procedure already applied in Refs. 6 and 15 was adopted also in the present case. In particular, the fit model contains one central Lorentzian function, globally accounting for the quasielastic contributions, and a damped harmonic oscillator (DHO) modeling of the inelastic component. In formulas:

$$S(Q,\hbar\omega) = S_{qe}(Q,\omega) + S_{\text{in}}(Q,\omega) = [n(\omega) + 1]$$
$$\times \left[\frac{\hbar\omega}{k_B T} \frac{a_0(Q)\,\Gamma_0(Q)}{\pi\left[\omega^2 + \Gamma_0^2(Q)\right]} \right.$$
$$\left. + \frac{a_c(Q)\,\Gamma_c(Q)\omega}{\left[\omega^2 - \omega_c^2(Q)\right]^2 + [\Gamma_c(Q)\omega]^2} \right], \quad (1)$$

where $n(\omega)$ is the Bose factor, and $\Gamma_0(Q)$, $\Gamma_c(Q)$, $\omega_c(Q)$, $a_0(Q)$, and $a_c(Q)$ were left as free parameters. The convolution of $S(Q,\hbar\omega)$ of Eq. (1) with the four-dimensional $(\mathbf{Q},\omega)$-dependent resolution function was actually fitted to the experimental data. The curves displayed in Fig. 1 witness the very good quality of the fits which provide a reduced χ^2 always very close to unity. The quasielastic contribution is modeled here using a very simple function because the energy resolution does not allow for a more detailed description of the central line, made up of both coherent and incoherent contributions. Actually, the width $\Gamma_0(Q)$ derived from the fit is in fair agreement with the NMR diffusion constant[17] and incoherent neutron scattering data.[18]

Further physical information can be obtained from the parameters $\hbar\omega_c(Q)$ and $\hbar\Gamma_c(Q)$ which provide the *unrelaxed* dispersion curve of the collective excitation and its damping parameter which is equal to the FWHM in the limit of small damping, i.e., when $\Gamma_c(Q) \ll \omega_c(Q)$. Considering that the determination of these two parameters is a delicate task, we made all possible tests to be sure that we were determining $\hbar\omega_c(Q)$ and $\hbar\Gamma_c(Q)$ with enough accuracy, and that no artifact was induced by our fitting procedure. The fit at low Q is accurate as we used different algorithms to perform the fit of the model and, at low momentum, the stability of the fit is undisputable. Indeed, we checked the relative coupling of the two parameters $\Gamma_c(Q)$ and $\omega_c(Q)$ by looking at the correlation matrix deduced from the fit when $Q \leqslant 0.7$ Å^{-1}. This matrix is almost diagonal, indicating that the two parameters are independent of each other and that the χ^2 minimum is well defined, thus providing a good estimate of the parameters and their errors. Upon increasing Q, the dynamic structure factor collapses into a rather broad distribution, as was already observed in previous investigations,[6,14,15] but it is evident from the data that the energy range we explored is adequate for comparing the model and the experimental data.

The final results of the fit, that is the dispersion curve $\hbar\omega_c(Q)$ and the damping parameter $\hbar\Gamma_c(Q)$, are plotted in Fig. 2. We see that $\hbar\omega_c(Q)$ shows the anomaly already observed[6,14,15] at $Q = 0.8$ Å^{-1}, while in the same momentum range $\hbar\Gamma_c(Q)$ shows a rather sharp increase when compared to a linear extrapolation from the low Q data. In this higher Q range, there is a correlation between the two parameters $\hbar\omega_c(Q)$ and $\hbar\Gamma_c(Q)$, but there is no reason for an abrupt change of one of them since this correlation appears smoothly
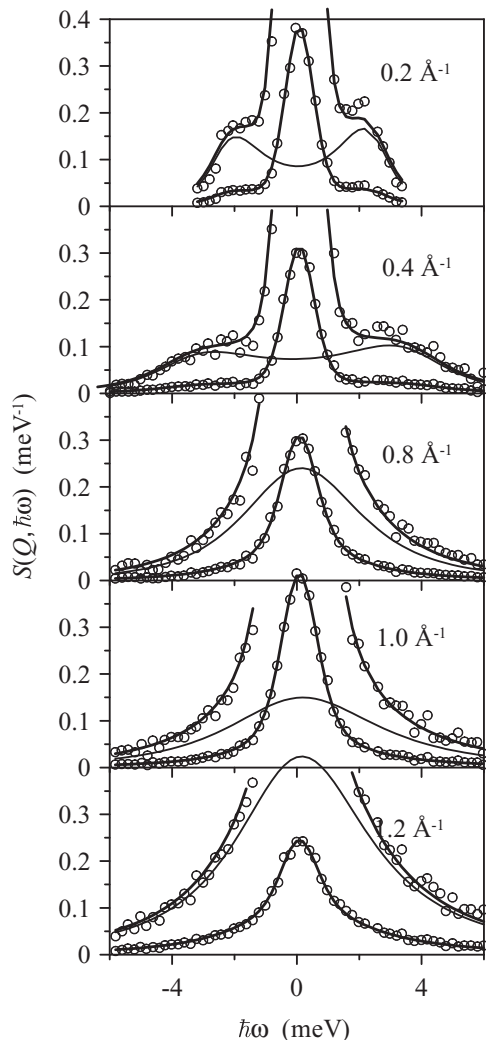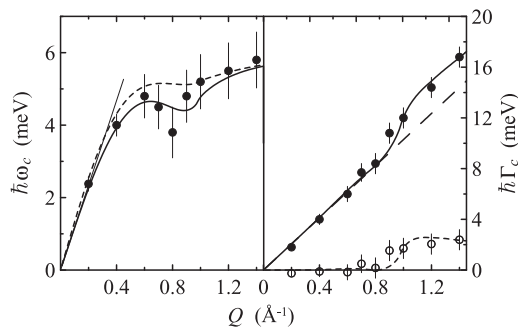
FIG. 2. Left panel, experimental dispersion curve (full circles) deduced from the fits of Eq. (1). The best-fit curve (solid line) according to the model described in the text is compared with the RPA result (dashed line). The thin straight line through the origin is the $Q \to 0$ behavior $\omega = c_s Q$, with a fitted c_s value of 1780 m/s. Right panel, experimental damping (full circles), fit of the model described in the text (full line), linear contribution from the fit (long dashed line), difference between experimental data and linear contribution (circles) and corresponding quantity from the fit results (dashed line).

as the spectrum broadens upon increasing Q. Moreover, this anomalous behavior is actually present in the $S(Q,\hbar\omega)$ data themselves. Indeed, when the experimental second frequency moment of the dynamic structure factor, namely $\langle\omega^2\rangle = \int_{-\infty}^{+\infty} S(Q,\omega)\,\omega^2\,d\omega$, is determined, a clear dip in the range 0.8–0.9 Å^{-1} is observed. This behavior is shown in Fig. 3, where $\langle\omega^2\rangle$ is reported as a function of Q. In Fig. 3, the static structure factor[19] is also reported to show that the dip of $\langle\omega^2\rangle$ is not a mere structural effect, since the small pre-peak observed in $S(Q)$ in the same Q region is actually located at $Q \simeq 1.05$ Å^{-1}. Therefore, the abrupt change of $\langle\omega^2\rangle$ at $Q \simeq 0.8$ Å^{-1} has a dynamical origin. Further information can also be gained by looking at the Q dependence of the ratio $\Gamma_c(Q)/\omega_c(Q)$, which is reported in Fig. 4. A clear break is observed at $Q \simeq 0.8$ Å^{-1}, which enhances, in a different way, the trend of $\Gamma_c(Q)$.

An additional remark can be made about the model we adopted. The relevant statistical procedures have been employed to define the model function. There are two obvious choices: the present one based on the DHO, or an approach based on a sum of Lorentzian functions, which is appropriate
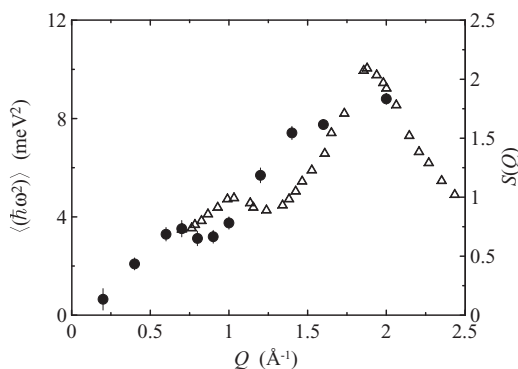

FIG. 3. Second moment of the dynamic structure factor from the present experiment as a function of Q (full circles), compared with the experimental $S(Q)$ deduced from neutron diffraction experiments (Ref. 19) (empty triangles).
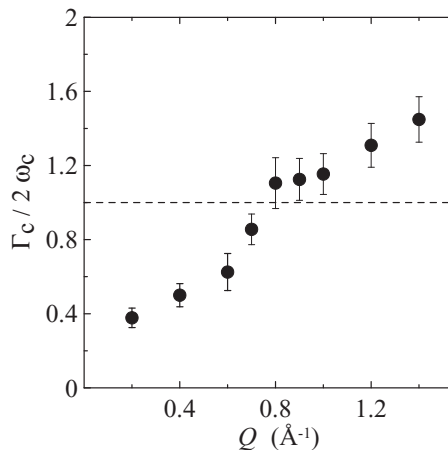

FIG. 4. Ratio of the damping parameter $\Gamma_c(Q)$ to the parameter $\omega_c(Q)$ which describes the dispersion curve (dots). The dashed line indicates the value of the ratio which corresponds to an overdamping of the collective modes.

in the quasielastic region. There is no doubt that at low Q the first one must be employed for the inelastic contribution. Upon increasing Q, there is no reason to change the model abruptly, however, for completeness, one can also check the validity of a model based on a sum of Lorentzian functions. For this check, we first applied the Bayesian analysis outlined by Sivia and used in different papers[20] to define the best number of Lorentzian functions. From the Bayesian method it results that two Lorentzians are the best choice. However, even if a slightly safer fit might be obtained using three Lorentzian components (the Bayesian analysis does not discriminate the two choices at best), it is found that this better fit occurs at the expense of losing the physical meaning of the parameters, because the intensity of the components turns out to be not positively defined.

Nonetheless, the validity of the DHO against the sum of Lorentzians is directly manifested by the high-Q experimental data themselves. Indeed, by plotting the experimental intensity above 4 meV, it is seen that the decreasing trend of the data is well accounted for by $S(Q,\omega) \propto \omega^{-3}$, the behavior expected for the DHO, rather than by $S(Q,\omega) \propto \omega^{-1}$, as expected for a Lorentzian modeling. These limit values are valid even taking into account the effect of the experimental resolution function and are obtained considering the product between the high energy limit of the model function and the appropriate detailed-balance factor $\beta\omega/[1 - \exp(-\beta\omega)]$. As an example, the tail of the experimental data at $Q = 2$ Å^{-1} and the fit curves corresponding to $S(Q,\omega) \propto \omega^{-3}$ and $S(Q,\omega) \propto \omega^{-1}$ are reported in Fig. 5 as a function of ω^{-3} and ω^{-1}, respectively. The latter fit provides a reduced χ^2 of 9.8 against the value of $\chi^2 = 1.4$ obtained with the ω^{-3} trend. A better agreement between ω^{-1} and the experimental data can be achieved only at the expense of subtracting from the data a quite unlike background, even if also in this case the fit favors the ω^{-3} trend.

For further consideration of the meaning of the fitting model, the energy integrals $Z_{qe}(Q)$ and $Z_{\text{in}}(Q)$ of, respectively, the two contributions $S_{qe}(Q,\omega)$ and $S_{\text{in}}(Q,\omega)$ in Eq. (1), are shown in Fig. 6, where the static structure factor $S_n(Q)$
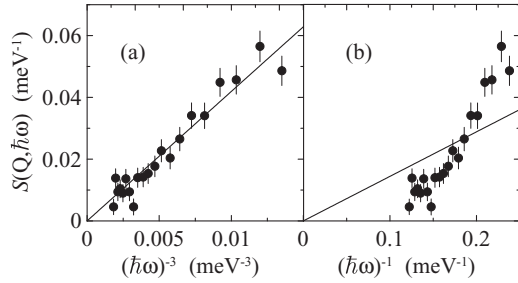
FIG. 5. Upper-energy tail (above 4 meV) of the experimental dynamic structure factor at $Q = 2$ Å^{-1} compared with a ω^{-3} (panel a) and a ω^{-1} (panel b) asymptotic behavior. The former corresponds to a DHO modeling, the latter to a Lorentzian description of the asymptotic inelastic (asymmetric) signal (see text). Data and fits are reported as a function of ω^{-3} in panel (a), and of ω^{-1} in panel (b).

determined by neutron diffraction[19] is also reported. It can be observed that $Z_{in}(Q)$ displays a relative maximum before the Q value at which a pre-peak is present in $S_n(Q)$. As already noted, the dispersion relation anomaly at Q_a and the small peak in $Z_{in}(Q)$ occur at the same Q value. Conversely, the pre-peak in $S_n(Q)$ is predominantly due to $Z_{qe}(Q)$, and is not related to $Z_{in}(Q)$. The decrease toward zero of $Z_{qe}(Q)$ at high Q is likely due to the merging of $S_{qe}(Q,\omega)$ and $S_{in}(Q,\omega)$, which the fit is unable to separate properly. No special meaning can be attributed to this detail: probably, the present data are such that, at high Q, it is not possible to distinguish between the quasielastic component and an overdamped DHO contribution. It is worth recalling that a modeling of the high-Q data by means of two Lorentzian functions provides in any case a worse fit than the DHO-based one, having the former a much lower probability according to Bayesian analysis.[20] Actually, the model we selected is able to provide a good description of the data with a minimum set of *a priori* assumptions.
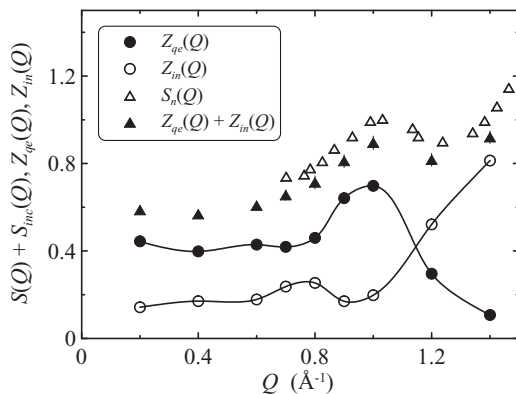

FIG. 6. Q dependence of the energy integral of the best-fit quasielastic (full circles) and inelastic (empty circles) components of Eq. (1), and of their sum (full triangles). The incoherent contribution $S_{inc}(Q)$ has been added to the experimental static structure factor obtained by neutron diffraction (Ref. 19), which is also shown (empty triangles). The error bars are smaller than the size of the symbols when not visible. The full lines are a guide to the eye.

III. RESULTS AND DISCUSSION

Starting from the results obtained from the present experimental data and model fitting procedures, we see that the low-momentum region, where the propagation is dominated by the long-range (screened) ion-ion interactions, the present data confirm the results of the previous neutron and x-ray studies.[6,15] The shortcomings of the interpretation proposed in Ref. 15 for the collective-mode velocity, based on an empirically adjusted screening wave vector in the equation for c, have been discussed in Ref. 6. Indeed, k_s^2 is known to be not positively defined so that it cannot be used as an adjustable parameter in the data analysis. Also, the finite ion-size effect must be considered since it plays quite some role.

At higher momentum transfers, a more complex trend in the dispersion curve is brought about by the dip clearly observed here around Q_a. Indeed, in our previous neutron investigation[6] the limited Q range did not allow for a detailed determination of the Q dependence of the collective mode energy. On the other hand, the x-ray measurements[14,15] were limited by the energy resolution, which was about twice the present one and not Gaussian-shaped. Here, the better energy resolution provides most reliable data for the interpretation of the high-Q collective behavior and enhances the unexpected trend seen in Fig. 2.

According to our previous work, the dispersion relation can be modeled as $\omega^2(Q) = \Omega_{ion}^2(Q) + \frac{Q^2}{4\pi e^2}|v(Q)|^2[1/\epsilon(Q) - 1]$, where $\Omega_{ion}^2(Q)$ is the dispersion of the ion plasma, $v(Q)$ is the electron-ion interaction, and $\epsilon(Q)$ is the electron gas dielectric function which screens the ion-ion interaction. The phenomenological form $\frac{Q^2}{4\pi e^2}|v(Q)|^2 = \Omega_p^2[1 - z_e(Q)]$, with $z_e(Q) = \alpha Q^2 \exp[-\beta Q^2]$, can be adopted to rewrite the dispersion relation assuming that $\Omega_{ion}^2 \approx \Omega_p^2$. This leads to $\omega^2(Q) \approx \Omega_p^2\{z_e(Q) + [1 - z_e(Q)]/\epsilon(Q)\}$. The above schematization can then be used to model the dispersion curve, with α and β left as adjustable parameters, and the (static) dielectric function estimated from QMC simulation results[12] using the procedure described in Ref. 6. As is seen in Fig. 2, a good fit of the experimental data is obtained with $\alpha = 4.30$ Å^2 and $\beta = 2.45$ Å^2, while keeping Ω_p fixed at the value deduced from the density and mass of the Li(ND$_3$)$_4$ complex with unit charge.

The crucial role of the dielectric function is elucidated by the curves reported in Fig. 7. Clearly, the anomaly at $Q \simeq Q_a$ is dominated by the behavior of $\epsilon(Q)$, which is negative up to Q_a. It is also evident how an RPA approach in the calculation of $1/\epsilon(Q)$ is unable to account for the experimental data, since it is always positive. Finally, we observe that the present β value corresponds to an ion diameter of about 3.8 Å, which compares with the size of Li(ND$_3$)$_4$ complex.[19]

Concerning the damping of the collective modes, a rather abrupt increase of the mode width is seen above Q_a. This particular behavior actually suggests that at Q_a a *decay channel* for the collective mode opens. It is difficult to ascribe this decay channel to either the ion-ion anharmonic interactions or to structural relaxations, since $\Gamma_c(Q)$ changes rather abruptly.

To get an empiric description of the decay channel, we assume the presence of an interaction between collective
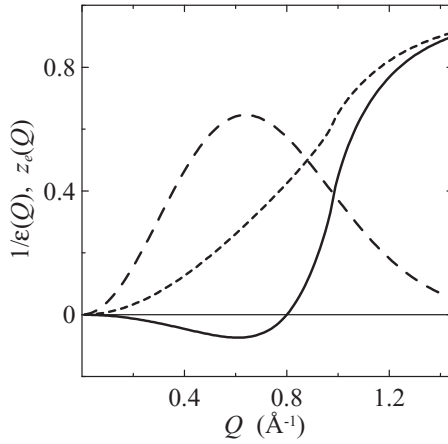
FIG. 7. Comparison among the Q dependencies of the inverse dielectric function $1/\epsilon(Q)$ (full line), its RPA estimate (dashed line), and $z_e(Q)$ (long dashed line).

modes and an additional electron gas mode, which models the increase of damping through the transition rate $w_f = \frac{2\pi}{\hbar} \rho_F \langle |V_{int}|^2 \rangle_T$, with ρ_F the density of final states, V_{int} the interaction matrix element, and $\langle \cdots \rangle_T$ the thermal average. Of course w_f measures the contribution to the collective mode inverse lifetime coming from the interaction with the decay channel. To lowest order, V_{int} can be taken to be linear in the ion displacement, i.e., linear in the collective mode annihilation and creation operators. The transition rate becomes $w_f \propto [Q\, v_s(Q)]^2 \{2n[\omega_c(Q)] + 1\}/\omega_c(Q)\{1/[(Q - \Re q_0)^2 + (\Im q_0)^2] + 1/[(Q + \Re q_0)^2 + (\Im q_0)^2]\}^2$, with $v_s(Q)$ the screened Coulomb interaction energy and q_0 the *complex* wave vector characterizing the additional electron-gas mode. At low Q values, w_f is expected to be small compared to frequency, since the above expression peaks at about q_0. We thus modeled the experimental $\Gamma_c(Q)$ as the superposition of a linear term in Q plus w_f. To enable comparison with the experimental data, we left the linear coefficient and q_0 as free parameters, while $v_s(Q)$ was calculated from the QMC prescription for $\epsilon(Q)$.[12]

The panel (b) of Fig. 2 shows how the proposed model accounts well for the experimental $\Gamma_c(Q)$. The present data are thus compatible with an electron density fluctuation having a complex wave vector $q_0 = [1.1 \pm 0.2 + i(0.8 \pm 0.2)] \cdot k_F$, with k_F the Fermi wave vector.

The origin of density fluctuations of the electron gas is difficult to retrace. Recently, it was suggested that in the low density region the electron gas can become unstable against the so-called damped charge density wave (DCDW).[21] It is therefore rather tempting to identify the decay channel emerging from our analysis as due to the interaction of the collective modes with a DCDW. This possibility is further suggested by the comparison with the theoretical result $q_0 = [1.43 + i0.96] \cdot k_F$ of Ref. 21, which is compatible with the present findings. One could also speculate about possible relationships between the present observation and the crystallization of the electron gas foreseen at the much lower electron densities attainable by computer simulations.

IV. CONCLUSIONS

We showed the importance of investigations of low electron-density systems, here found to open new perspectives for both theoretical and experimental research. This work evidences a precise role of the low-density electron gas on the ion dynamics of saturated lithium-ammonia, and highlights the crucial effects that the dielectric function has on the ion collective modes and their dispersion law. We believe that most of the effectiveness of the present analysis descends from a realistic treatment of the electron-gas properties, only made possible by the modern and quite refined QMC description of the (static) dielectric function. The proposed interpretation framework gives a very good account of the experimental results in the wider Q range here accessed, thus supporting the existence of interactions between ion- and electron-density fluctuations.

*Present address: ISIS Facility, Rutherford Appleton Laboratory, Chilton, Oxfordshire, OX11 0QX, UK.

[1] G. D. Mann, *Many-Particle Physics* (KluwerAcademic/Plenum, New York, 2000).

[2] N. H. March, *Liquid Metals* (Cambridge University Press, Cambridge, 1990).

[3] G. Ortiz, M. Harris, and P. Ballone, Phys. Rev. Lett. **82**, 5317 (1999).

[4] K. Tamura, K. Matsuda, and M. Inui, J. Phys. Condens. Matter **20**, 114102 (2008).

[5] L. E. Bove, F. Formisano, F. Sacchetti, C. Petrillo, A. Ivanov, B. Dorner, and F. Barocchi, Phys. Rev. B **71**, 014207 (2005), and references therein; W.-C. Pilgrim, M. Ross, L. H. Yang, and F. Hensel, Phys. Rev. Lett. **78**, 3685 (1997).

[6] F. Sacchetti, E. Guarini, C. Petrillo, L. E. Bove, B. Dorner, F. Demmel, and F. Barocchi, Phys. Rev. B **67**, 014207 (2003).

[7] A. A. Louis and N. W. Ashcroft, Phys. Rev. Lett. **81**, 4456 (1998).

[8] The value of n_c can be derived from the electron gas energy of Ref. 3.

[9] G. Giuliani and G. Vignale, *Quantum Theory of the Electron Liquid* (Cambridge University Press, Cambridge, 2005).

[10] O. V. Dolgov, D. A. Kirzhnits, and E. G. Maksimov, Rev. Mod. Phys. **53**, 81 (1981).

[11] C. F. Richardson and N. W. Ashcroft, Phys. Rev. B **50**, 8170 (1994), and references therein.

[12] S. Moroni, D. M. Ceperley, and G. Senatore, Phys. Rev. Lett. **75**, 689 (1995).

[13] T. Bodensteiner, Chr. Morkel, W. Glaser, and B. Dorner, Phys. Rev. A **45**, 5709 (1992).

[14] C. A. Burns, P. M. Platzman, H. Sinn, A. Alatas, and E. E. Alp, Phys. Rev. Lett. **86**, 2357 (2001).

[15] A. H. Said, C. A. Burns, E. E. Alp, H. Sinn, and A. Alatas, Phys. Rev. B **68**, 104302 (2003).

[16]M. J. Cooper and R. Nathans, Acta Crystallogr. **23**, 357 (1967); B. Dorner, Acta Crystallogr. A **28**, 319 (1972).

[17]A. N. Garroway and R. M. Cotts, Phys. Rev. A **7**, 635 (1973).

[18]H. Thompson, N. T. Skipper, J. C. Wasse, W. S. Howells, M. Hamilton, and F. Fernandez-Alonso, J. Chem. Phys. **124**, 024501 (2006).

[19]H. Thompson, J. C. Wasse, N. T. Skipper, S. Hayama, D. T. Bowron, and A. K. Soper, J. Am. Chem. Soc. **125**, 2572 (2003); J. C. Wasse, S. Hayama, N. T. Skipper, and H. E. Fischer, Phys. Rev. B **61**, 11993 (2000), and references therein.

[20]D. S. Sivia, *Data Analysis: A Bayesian Tutorial* (Clarendon, Oxford, 2005); F. J. Bermejo, W. S. Howells, M. Jiménez-Ruiz, M. A. González, D. L. Price, M. L. Saboungi, and C. Cabrillo, Phys. Rev. B **69**, 174201 (2004); F. Sacchetti, A. Orecchini, A. Cunsolo, F. Formisano, and C. Petrillo, *ibid.* **80**, 024306 (2009).

[21]A. M. J. Schakel, Phys. Rev. B **64**, 245101 (2001).